Key Engineering Materials
ISSN: 1662-9795, Vol. 813, pp 322-327
doi:10.4028/www.scientific.net/KEM.813.322

Submitted: 2019-04-12
Revised: 2019-05-24
Accepted: 2019-05-27
Online: 2019-07-22

Osteoblast Cell Response to LIPSS-Modified Ti-Implants

Leonardo Orazi[1,a], Maksym Pogorielov[2,3,b], Volodymyr Deineka[2], Evhenia Husak[2], Viktoriia Korniienko[2], Oleg Mishchenko[3], Barbara Reggiani[1,c]

[1]Dept. of Sciences and Methods for Engineering, University of Modena and Reggio Emilia, Reggio Emilia, Italy

[2]Medical Institute, Sumy State University, Sumy, Ukraine

[3]Osteoplant R&D, Debice, Poland

[a,*]leonardo.orazi@unimore.it, [b]m.pogorielov@gmail.com [c]barbara.reggiani@unimore.it

Keywords: nanotexturing, cell proliferation, bacteriology, HR-LIPSS, femtosecond laser

Abstract. In the present work, the surface of Ti-6Al-7Nb samples was patterned with Laser Induced Periodic Surface Structures in order to improve biocompatibility, increase tissue ingrowth and decrease bacterial adhesion and inflammatory response for applications in dental and orthopedic implants. Polished and sandblasted disks 10 mm in diameter were treated generating LIPSS under two different sets of parameters. The surface morphology and chemistry were investigated both by secondary electrons imaging, EDS analysis and Atomic Force Microscopy. Primary rat osteoblast culture (passage 2) was used to assess cell toxicity and biocompatibility. Alamar Blue assay was used to access cell viability and proliferation on day 1, 3 and 7. The difference between cell adhesion on polished and sandblasted surface as well as between polished and LIPSS-modified surface are described and discussed.

Introduction

Prevalence of age-related diseases and increase in life expectancy, as well as advantages in surgical techniques, lead to intensive worldwide increasing of bone replacement and reconstructive procedure. More than 1 million arthroplasty performed annually in EU and projections indicate that the number of primary and revision joint arthroplasties will grow significantly in coming years [1]. However, a need of revision as high as 17.5% after bone replacement surgery is reported [2]. Incomplete osteointegration and microbial infection represent the major contributions in implant failure. Microbial populations use cell attachment to solid substrates to survive, forming biofilms [3]. An efficient approach to prevent the biofilm formation consists in depositing a bactericidal layer on the material's surface. However, depending on the application, this approach is not completely satisfactory because of its limited efficiency, toxicity or due to its role in the emergence of multiresisting pathogens [4][5].

A possible solution is offered by surface modifications able to improve implant osteointegration or reduce bacterial infection operating both on morphology [6] and microstructure and chemistry [7]. In this context, in the last years, laser processing techniques gained a lot of attention as methods to enhance the biocompatibility for implant surfaces. In [8] CO_2 laser texturing was employed to enhance tribological performances and proliferation of MG63 cells on Ti6Al4V. Authors observed a strong influence of the surface aspect ratio both on cell proliferation and tribological performances. Pulsed fiber laser with a wavelength of 1064 nm and operating at 10 ns was used in [9] to generate grooves on NiTi alloy, the differently spaced lines grid influences the proliferation and notably the orientation of human mesenchymal stem cells. In laser texturing obtained with continuous or pulsed lasers the minimum dimension of the features are limited by the diffraction law, making very difficult to obtain grooves or craters with dimensions below 10 μm. However, in the last years, a new approach based on the use of ultrashort pico and femtosecond laser was developed. This method allows to generate, on the surface, the so-called LIPSS (Laser Induced Periodic Surface Structures). These periodic morphological reliefs are characterized by a periodicity usually in the range 500-900 μm always lower than the laser wavelength [10]. this opens interesting perspectives to modulate surface

wettability [11], [12] to enhance the proliferation or the viability of cells [13] or to reduce the resistance of surface to bacterial proliferation [14].

The aim of the present work is to investigate how LIPSS based surface treatments of Ti6Al7Nb samples modify osteoblast proliferation and S. aureus bacterial adhesion.

Materials and Methods

Rods of Ti-6Al-7Nb were cut generating disks 10 mm in diameter and 5 mm in height. 60 samples were mechanically polished while the others were sandblasted following methods and procedures of the production line of certified prosthesis and implants.

Samples were divided in 6 groups, 20 samples each. The laser treatments were performed by a Coherent HyperRapid NX laser, operating at 1064 nm with pulse duration of about 8 ps. Samples surface was scanned by a Raylase Focusshifter CS scanner equipped with a 160 mm focal length lens. The focused spot, measured with a beam analyzer, presented a diameter of about 30 μm. The first treatment (Text1) was carried out with a pulse energy of 16 μJ and an overall dose of 27 J/cm^2 while in the second treatment condition (Text2) the pulse energy was 32 μJ and the overall dose was 270 J/ cm^2.

Table 1 Samples labelling

	Untreated	Laser parameter Text1	Laser parameter Text2
Polished	*NT-Polished*	*LIPSS-Text1-Polished*	*LIPSS-Text2-Polished*
Sandblasted	*NT-SB*	*LIPSS-Text1-SB*	*LIPSS-Text2-SB*

After the laser treatments, all the samples were prepared for the biological essays by washing in ultrasonic bath and sterilization with gamma ray. All media and reagents for cell culture were purchased from Gibco® (USA) while all bacteriological media were purchase from HiMedia (India). All cell lines used in the experiments (human osteoblast) were taken from cell collection of Sumy State University while bacterial culture were obtained from 'Bacteriological Museum of Sumy State University'. The experiments were carried out in Certified Class 2 Laboratory in Medical Institute of SSU. All experimental *in-vitro* procedures were approved by the Institutional Ethic Committee (Sumy State University).

The cells were grown in 75 cm^2 tissue culture flasks under standard culture conditions of 5% CO_2 humidified air at 37 ^{0}C with medium renewal for every 2–3 days. Dulbecco's Modified Eagle Medium/Nutrient Mixture F-12 (DMEM/F-12) with L-glutamine used, containing 100 units/ml penicillin, 100 μg/ml streptomycin, 2.5 μg/ml amphotericin B, 10% Fetal Bovine Serum and 1.0 ng/ml bFGF. After removing medium, osteoblasts were seeded on each samples and positive control wells at a cell density of 2×10^4 cells per well.

Osteoblast cells adhesion at 24 hours and cell proliferation on scaffolds were assessed by the Alamar blue colorimetric assay, which is used to measure cell viability. Alamar blue (Invitrogen) were added in an amount equal to 10% of the volume to each well. As negative control, Alamar Blue solution was added to the medium without cells. As positive control Alamar blue solution was added to the medium which wells contains only cells without samples. The plates were incubated for 4 hours at 37°C, in the dark. The medium was transferred to another 96-well plate and absorbance was measured using a Multiskan FC (Thermo Fisher Scientific) plate reader at wavelengths of 570 nm and 600 nm. The cells were quantified at different time intervals: 1 day, 3 days and 7 days. All experiments were repeated 7 times. The percentage of Alamar blue reduction was computed according to the manufacturer's protocol.

The adhesive properties of the differently processed disks were assessed on gram-positive bacterium (S. aureus, strain B 918). The bacterial strain grown on nutrient agar at 37 °C for 24 h was suspended in a saline solution (0.9 %, w/v NaCl) and re-suspended to a final density of $1x10^5$ colony forming units (CFUs)/mL (5 log CFU) in nutrient broth using McFarland standards.

The disks were incubated horizontally with 2.0 ml of the bacterial suspension in static conditions in a 24-well plate at 37 °C for 2, 4, 6 and 24 h. Then, the specimens were removed with sterile forceps

and washed with 2.0 ml sterile physiological saline three times to remove freely-adherent bacteria. After that, disks were placed in sterile tubes with 1.0 ml of sterile saline solution, and sonicated for 1 min by using an ultrasonic-bath (B3500S-MT, Bransone Ultrasonics Co., Shanghai, China) to purge out adherent bacteria from the surfaces of the specimens. Following this, the colony count at each term of incubation was conducted using streak plate technique cultivating 10 µl aliquots saline solution from sonicated tubes onto the solid media for 24 h. The wells containing disks and tested samples in growth medium without bacterial inoculate were used as a control. All experiments were replicated three times. One-way ANOVA with multiple comparisons was used to assess difference between groups using GraphPad Prism 8.0 software. Statistical significance was assumed at a confidence level of 95% ($p < 0.05$).

Results

The surface morphology after laser pattering was evaluated by SEM analyses (Fig. 1).

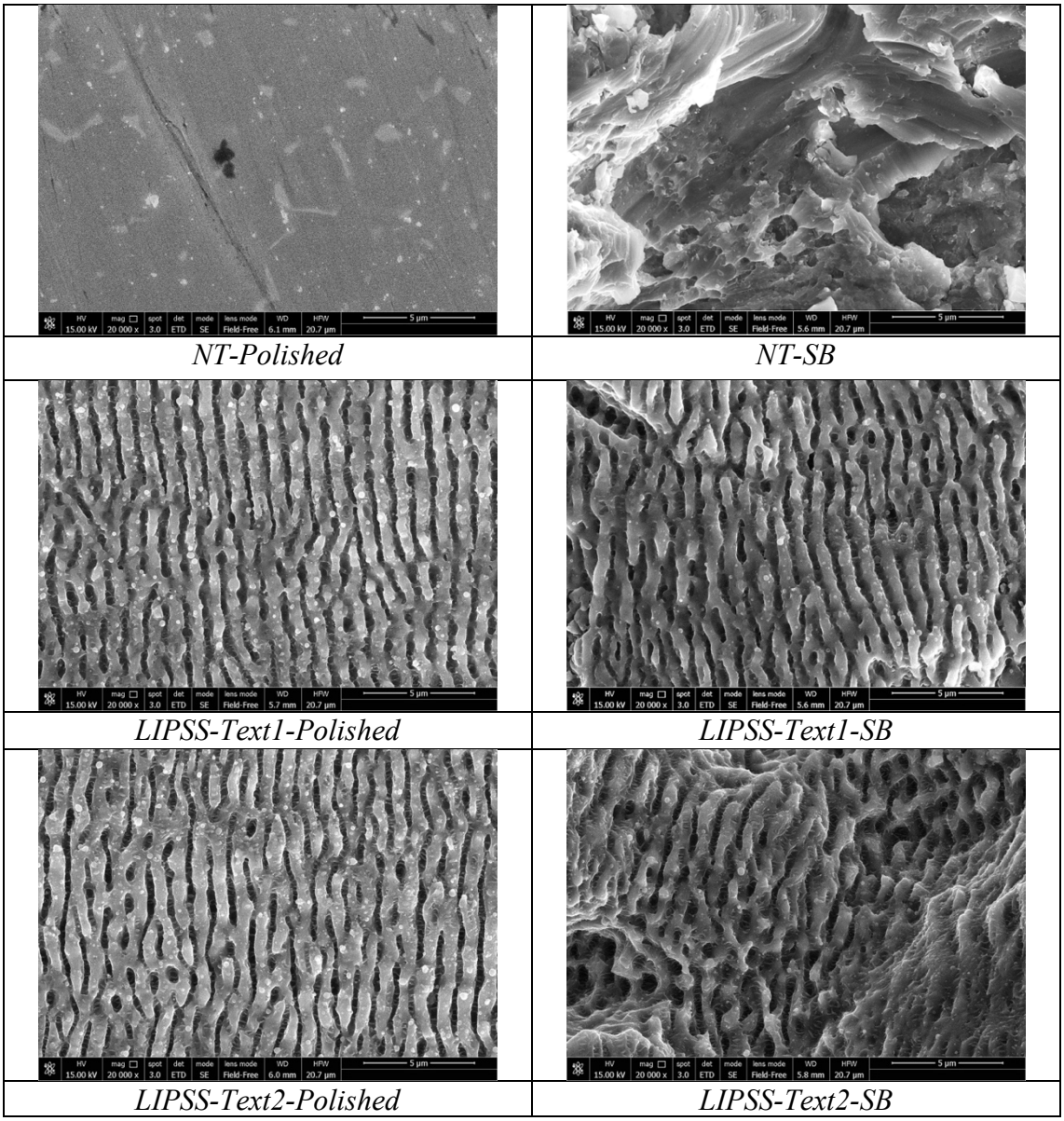

Figure 1. SEM images (20000x) representing the surface morphology under different treatments.

The images in the first row show untreated samples surface, in particular in image coded *NT-SB* the ploughing action and the severe deformation induced by the abrasive is clearly evident. It is not easy to define an average dimensions of the "valleys" induced by the sand-blasting but it can be estimated in the order of tens of micrometers.

LIPSS on both the polished surfaces are quite uniform and homogeneous with some bifurcations. The direction of LIPSS is controlled by orienting the laser polarization plane. As possible to see in Fig. 2, in the valley of the LIPSS several HSFL (High Spatial Frequency LIPSS) are present. They are perpendicularly oriented with respect to the others and dimensions and periodicity are in the order of 100-200 nm. The same figure evidences the presence of material nanoparticles constituted by ablated materials that, from the plasma and vapor phase, re-solidified after touching the sample surface as melted drop.

The treatment of the sandblasted surfaces evidences the overlapping of LIPSS with the pre-existing morphology except in very hollow and narrow valley where diffraction blocks the entrance of the laser energy. The surface of *LIPSS-Text2-SB* treated samples are smoother due to the high quantity of energy deposited per surface unit resulting in some melting.

While the two laser treatments appear to substantially generate the same structures, a more detailed analysis of the periodicity shown in Table 2 evidences some differences.

Table 2 Average periodicity and relative dispersion

	LIPSS-Text1-Polished	*LIPSS-Text2-Polished*	*LIPSS-Text1-SB*	*LIPSS-Text2-SB*
Average period [nm]	959	812	1006	1006
Standard deviation [nm]	44	161	317	257

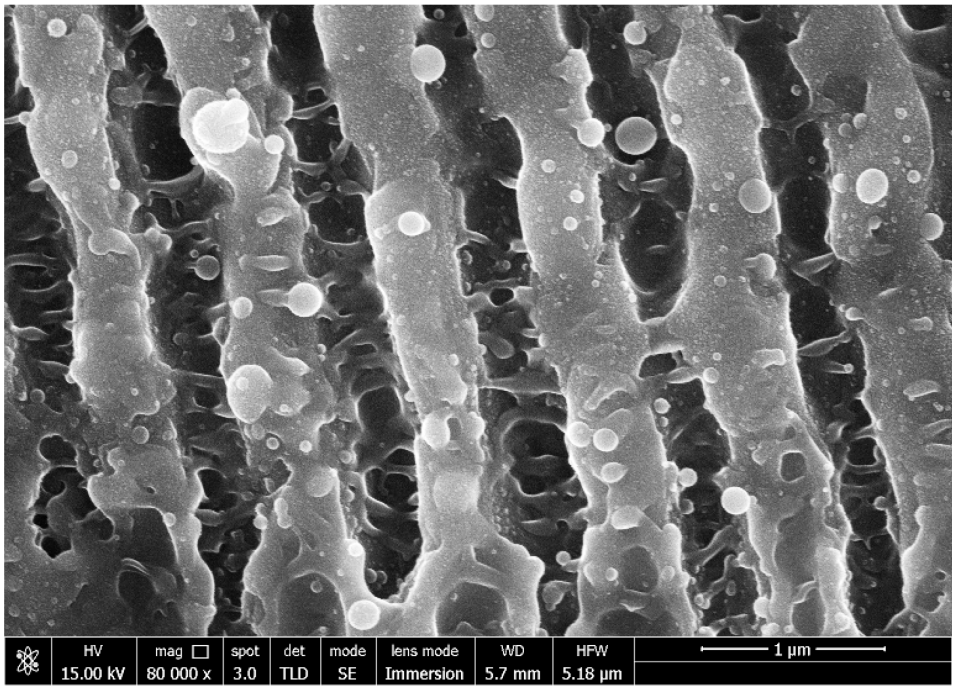

Figure 2. High magnification image of obtained LIPSS. HSFL are present in the valleys while some nanoparticles due to material recasting are stuck on the peaks.

The cell viability assay did not show cell toxicity of all surfaces, but the attachment and proliferation rates were significantly different, depending on surface modification. Cell adhesion on day 1 to polished surface was relatively weak – 35.29±1.89% and increase significantly in sandblasted group – 60.43±2.63%. *LIPSS* treatment of polished surface in both regimes significantly increase cell adhesion up to 45.0±1.91% ($p \leq 0.0001$) (*LIPSS-text1-Polished*) and 50.29±2.87% ($p \leq 0.0001$) (*LIPSS-text1-Polished*) but did not affect adhesion rate on sandblasted surface (figure 1). Proliferation assay on day 3 and 7 shown progressive cell growth on NT-SB and all LIPSS surfaces. It should be noted, that on day 3 we did not see significant difference in cell viability between *NT-SB* and polished *LIPSS-text1-Polished* and *LIPSS-text2-Polished*. We also do not find difference between *LIPSS* polished and sandblasted surfaces. Probably nano-patterning plays the main role in cell attachment and proliferation. On day 7 cells intensively proliferate both on sandblasted and all *LIPSS* surfaces but

we do not see difference in cell viability between *NT-SB* and *LIPSS-text1-Polished*. Number of viable cells on *LIPSS-text2-Polished* (98.71±1.89), *LIPSS-text1-SB* (94.43±2.99) and *LIPSS-text2-SB* (99.29±1.49) are significantly higher compared to *NT-Polished, NT-SB* and *LIPSS-text1-polished* ($p \leq 0.0001$).

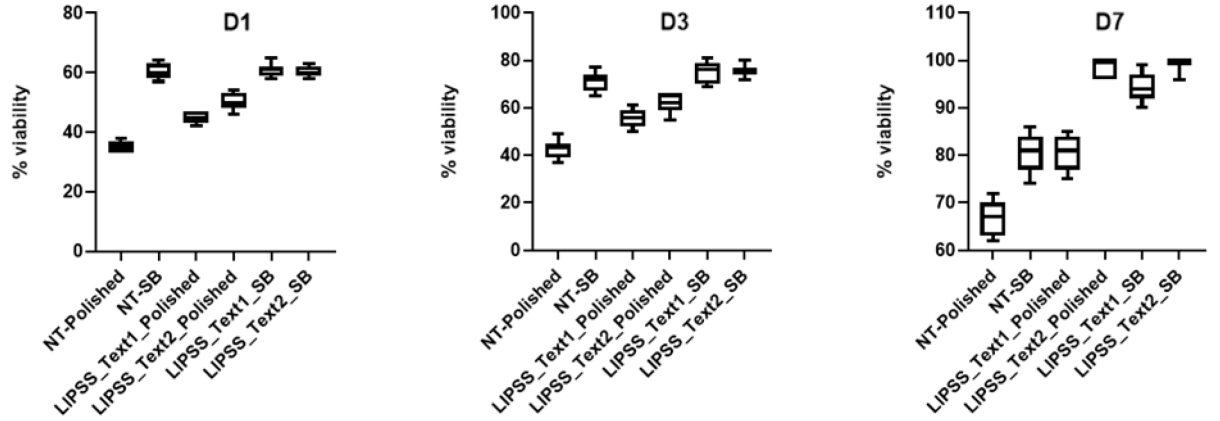

Figure 3. Cell viability assay in 1, 3 and 7 days after osteoblast seeding on non-treated and LIPSS-modified Ti surfaces.

No bacterial cells were found in 2 hour in polished surface, but in rest time-point intensive adhesion was detected with proliferation in 24 hours. The *NT-SB* and all *LIPSS-polished* surfaces show a bacterial cell adhesion lower than 2.0 log10 CFU compared to 5 log10 CFU of *NT-polished one*. The *LIPSS-text1-polished* surface keep antiadhesive properties within all time-points but *LIPSS-text2-polished* shows intensive bacteria attachment in 4-24 hours (Fig. 4). The similar results we can see on *LIPSS-text2-SB* implants. At the same time, *LIPSS-text1-SB* shown absence of bacteria attachment in 2, 4 and 6 hours and only long-time co-cultivation leads to loss of antiadhesive properties.

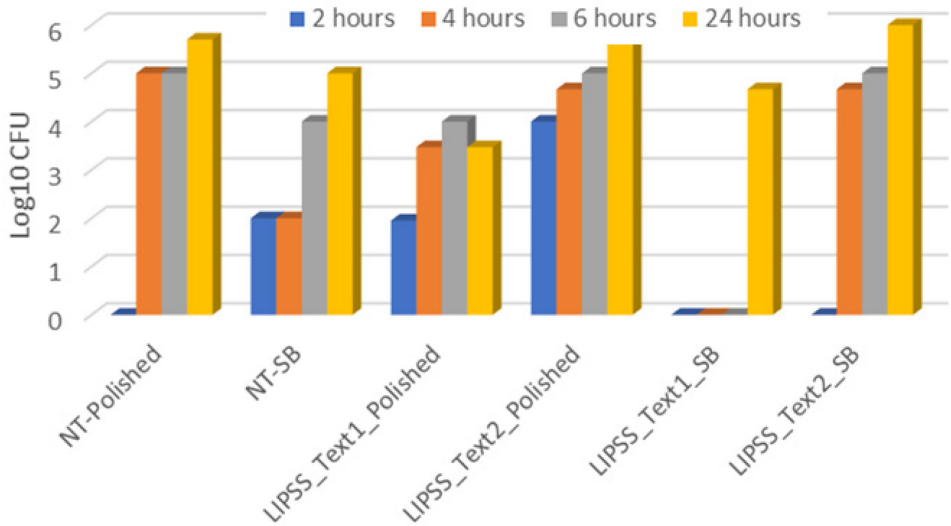

Figure 4. Number of bacterial cells (in Log10 CFU) adhered to implant surface in different time-points of co-cultivation.

Conclusions

The formation of linear periodic surface structures on Ti-alloy surface increases osteoblast cell adhesion and proliferation especially on polished implants. Proliferation rate significantly increases in both polished and sandblasted surfaces with LIPSS. This could enhance osteointegration performance of medical implants. *LIPSS-1* regime prevents bacterial cells adhesion within first 6 hours after co-cultivation and does not affect osteoblast cell adhesion. This can be used for development of high effective implant surface with osteogenic/antibacterial properties.

Acknowledgments

Authors would like to thank C.B. Ferrari srl (IT) for the practical execution of laser patterning. Biological investigations provided with support of H2020 MSCA-RISE NanoSurf 777926 project.

References

[1] L. Leitner *et al.*, "Trends and Economic Impact of Hip and Knee Arthroplasty in Central Europe: Findings from the Austrian National Database," *Sci Rep*, 8/1, p. 4707, (2018).
[2] S. Kurtz, F. Mowat, K. Ong, N. Chan, E. Lau, and M. Halpern, "Prevalence of Primary and Revision Total Hip and Knee Arthroplasty in the United States From 1990 Through 2002," *JBJS*, 87/7, p. 1487, (2005).
[3] A. P. V. Colombo and A. C. R. Tanner, "The Role of Bacterial Biofilms in Dental Caries and Periodontal and Peri-implant Diseases: A Historical Perspective," *J Dent Res*, 98/4, pp. 373–385, (2019).
[4] J. A. Lichter and M. F. Rubner, "Polyelectrolyte Multilayers with Intrinsic Antimicrobial Functionality: The Importance of Mobile Polycations," *Langmuir*, 25/13, pp. 7686–7694, (2009).
[5] A. Kulkarni Aranya, S. Pushalkar, M. Zhao, R. Z. LeGeros, Y. Zhang, and D. Saxena, "Antibacterial and bioactive coatings on titanium implant surfaces," *J Biomed Mater Res A*, 105/ 8, pp. 2218–2227, (2017).
[6] C. N. Elias, J. H. C. Lima, M. P. da Silva, and C. A. Muller, "Titanium Dental Implants With Different Morphologies," *Surf Eng*, 18/1, pp. 46–49, (2002).
[7] C. L. B. G. Neto, M. A. M. da Silva, and C. Alves, "Osseointegration evaluation of plasma nitrided titanium implants," *Surf Eng*, 25/6, pp. 434–439, (2009).
[8] M. Sadeghi, M. Kharaziha, H. R. Salimijazi, and E. Tabesh, "Role of micro-dimple array geometry on the biological and tribological performance of Ti6Al4V for biomedical applications," *Surf Coat Tech*, 362, pp. 282–292, (2019).
[9] R. Zhou, X. Lu, S. Lin, and T. Huang, "Laser texturing of niti alloy with enhanced bioactivity for stem cell growth and alignment," *J Laser Micro Nanoeng*, 12/1, pp. 22–27, (2017).
[10] I. Gnilitskyi, T. J.-Y. Derrien, Y. Levy, N. M. Bulgakova, T. Mocek, and L. Orazi, "High-speed manufacturing of highly regular femtosecond laser-induced periodic surface structures: physical origin of regularity," *Sci Rep*, vol. 7, no. 1, p. 8485, (2017).
[11] A. Cunha, A. P. Serro, V. Oliveira, A. Almeida, R. Vilar, and M.-C. Durrieu, "Wetting behaviour of femtosecond laser textured Ti–6Al–4V surfaces," *App Surf Sci*, 265, pp. 688–696, (2013).
[12] L. Orazi, I. Gnilitskyi, and A. P. Serro, "Laser Nanopatterning for Wettability Applications," *J. Micro Nano-Manuf*, 5/2, pp. 021008-021008–8, (2017).
[13] I. Gnilitskyi, M. Pogorielov, D. Dobrota, R. Viter, L. Orazi, and O. Mischenko, "Cell and Tissue Response to Modified by Laser-induced Periodic Surface Structures Biocompatible Materials for Dental Implants," in *Conference on Lasers and Electro-Optics, AW4O.6*, (2016).
[14] A. Cunha *et al.*, "Femtosecond laser surface texturing of titanium as a method to reduce the adhesion of Staphylococcus aureus and biofilm formation," *App Surf Sci*, 360, pp. 485–493, (2016).